INTERNATIONAL CENTRE FOR THEORETICAL PHYSICS (library stamp)

INTERNATIONAL ATOMIC ENERGY AGENCY
UNITED NATIONS EDUCATIONAL, SCIENTIFIC AND CULTURAL ORGANIZATION

INTERNATIONAL CENTRE FOR THEORETICAL PHYSICS
34100 TRIESTE (ITALY) - P.O. B. 586 - MIRAMARE - STRADA COSTIERA 11 - TELEPHONES: 224281/2/3/4/5/6
CABLE: CENTRATOM - TELEX 460392 - I

SMR/115 - 16

WINTER COLLEGE ON LASERS, ATOMIC AND MOLECULAR PHYSICS

(21 January - 22 March 1985)

ORDER AND CHAOS IN QUANTUM OPTICS

F.T. ARECCHI
Istituto Nazionale di Ottica
& Università di Firenze
Largo E. Fermi, 6
50125 Firenze
Italy

These are preliminary lecture notes, intended only for distribution to participants
Missing or extra copies are available from Room 229.

Acta Physica Austriaca 56, 57–74 (1984)

Acta Physica Austriaca

© by Springer-Verlag 1984

①

Order and Chaos in Quantum Optics*

By

F. T. Arecchi
Istituto Nazionale di Ottica, Università di Firenze, Italy

With 10 Figures

(Received June 6, 1984)

Summary

This paper is a critical review of the most challenging area of nonequilibrium statistical mechanics, namely the insurgence of ordered structures starting from a chaotic (maximum entropy) condition, in a system strongly perturbed at its boundary as a quantum optical system. For still higher perturbations, the ordered structures become more and more complex, until they resemble a chaotic situation (deterministic chaos, or turbulence). This turbulent regime is however rich in relevant information. Criteria for sorting this information are given.

1. Order from Chaos–Role of Nonlinearities and Role of the Boundary–The Laser

A detailed experimental analysis of the onset of order in a pumped system was given in my 1965–1967 investigations on the passage from incoherent to coherent light in a laser [1]. Fig. 1 shows the photon statistics (P.S.) for a radiation field below and above the threshold point (that is, the point where the gain provided by the stimulated emission processes of excited atoms compensates for the losses due to the escape of radiation from laser volume). The G curve is fitted by a Bose-Einstein distribution describing the fluctuations of the photon number in a black-body around the average value $\langle n \rangle$ given by Planck's formula, the L curve is fitted by a Poisson distribution. The two distributions correspond to fields with the same color, direction and intensity, so that there is no classical optics measurement which could discriminate between

* Invited lecture presented at the seminar on "Fundamentals of Quantum Optics" in Obergurgl, Austria, 1984.

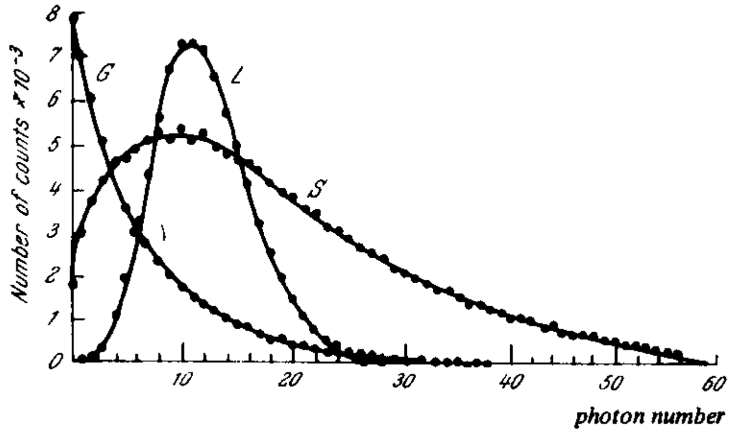

Fig. 1. Photocount distributions of three radiation fields. L laser field, G Gaussian field, S linear superposition with L and G onto the same space mode

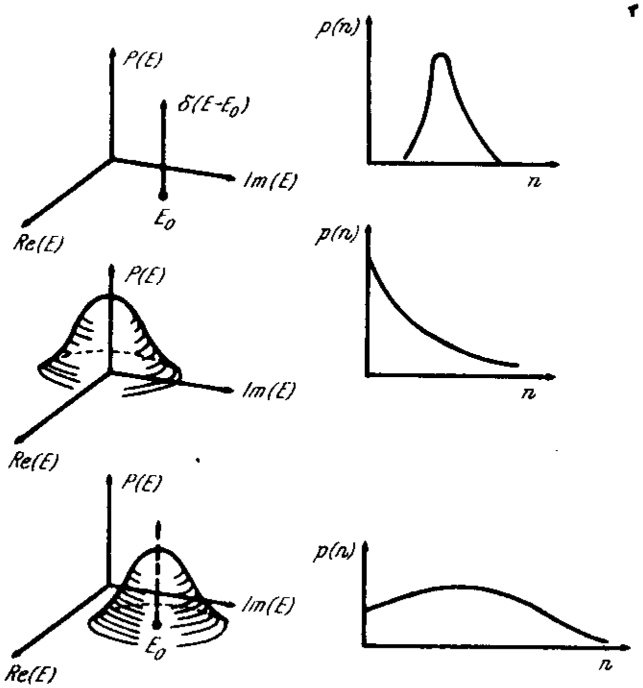

Fig. 2. Field and photon statistical distributions for an ideal coherent field (no fluctuations), for a thermal equilibrium field (Gaussian with zero average), and for the superposition of the two shifted Gaussian

them. Yet the P.S. measurement shows a dramatic difference. The why is given in Fig. 2. For a uniform field, since photons are Bose particles with zero mass, and hence delocalized, the associated photon detection processes at different points in space-time have no correlations. Therefore, in a volume filled with a coherent, or ordered, field (that is, a field with a δ-like statistics as in Fig. 2a), the associated probability $p(n)$ of detecting photons at a given point over a time T is a Poisson distribution.

If now the field has a zero-average Gaussian distribution, as for a thermal equilibrium or maximum entropy situation, weighting each probability element with the detection statistics one obtains the Bose-Einstein distribution. Between these two limit cases of full order and maximum chaos, one can trace a continuous manifold of intermediate cases (Fig. 2c). This smooth behavior is analogous to a second order phase transition, as a thermodynamic system undergoes a continuous change of state around a critical temperature. The explanation implies the essential role of nonlinearities. The elementary description of a laser in terms of Einstein stimulated emission processes compensating for losses is not sufficient. Indeed, this would just provide a linear polarization $P = \chi E$, and a quadratic free energy

$$F(E) = -P \cdot E = -\chi E^2. \tag{1}$$

In a thermodynamic system open with respect to the variable E, E has a statistical distribution given by

$$W(E) = N \exp[-F(E)/kT] \tag{2}$$

(N = normalization constant). Similarly a nonequilibrium system with a dynamical variable E, driven by a nonlinear force $f(E)$ and by stochastic noise with short correlation time and correlation amplitude D, has a stationary distribution [2, 3]

$$W(E) = N \exp\left[\int f(E)\, dE/D\right]. \tag{3}$$

In the absorbing case (force of the field proportional to the polarization $P = -\alpha E$; $\int f(E)\, dE = -\frac{1}{2}\alpha E^2$) by (3) the field has a Gaussian stationary distribution, as it should be expected from thermodynamics (2). In the linear emitting case the distribution is undefined ($P = \alpha E$; $\exp(\alpha E^2)$ is not normalizable). But an atom is still exposed to photons after emission. The lowest correction is cubic in the field (Fig. 3) and it is sufficient to describe the passage from Gaussian chaos to a narrow distribution around nonzero fields

$$\pm E_0 = \pm\sqrt{\alpha/\beta}. \tag{4}$$

The spontaneous symmetry breaking does not assign the phase of E_0.

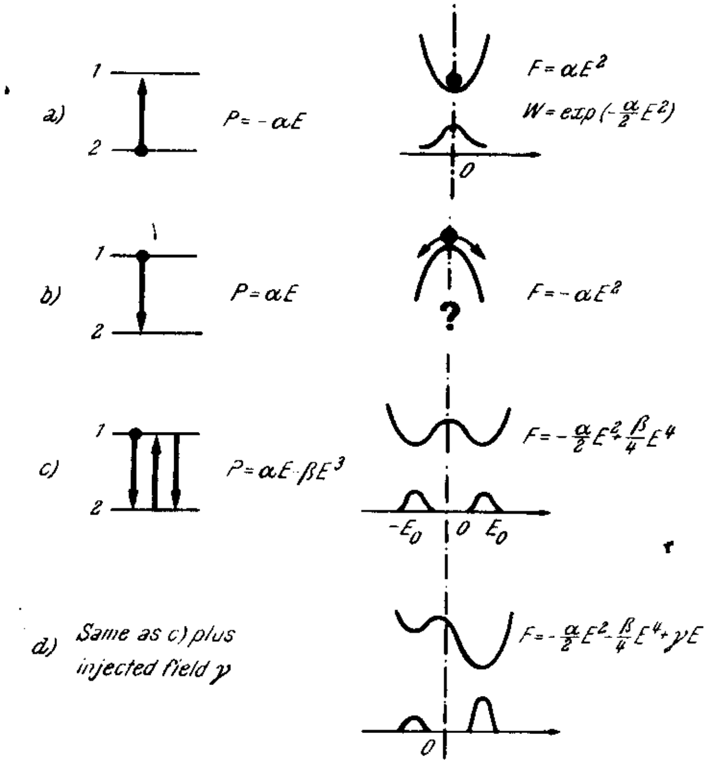

Fig. 3. *a* Absorbing atom, linear polarization; parabolic pseudo-potential; Gaussian probability. *b* Emitting atom, linear polarization; parabolic pseudo-potential; undefined probability. *c* Emitting atom, cubic polarization; quadratic pseudo-potential; probability peaks around coherent values $\pm E_0$. *d* As *c* but with a symmetry-breaking odd term in potential, arising from an external field

We have two equivalent states 180° apart. To lift the degeneracy we must apply an external field γ, which assigns a reference phase. The two states are no longer equivalent (optical bistability).

Fig. 4 shows the analogy with a thermodynamic phase transition. Here the order parameter is called q, and the control parameter is the temperature. In the Landau model, the coefficient of the quadratic term in the free energy

$$F(q) = \alpha q^2 + \beta q^4 \tag{5}$$

scales linearly with the temperature $\alpha = a(T - T_c)$, going through zero for the critical temperature T_c. In the laser case, q is the e.m. field E, and the control parameter is the difference N between excited atoms and ground

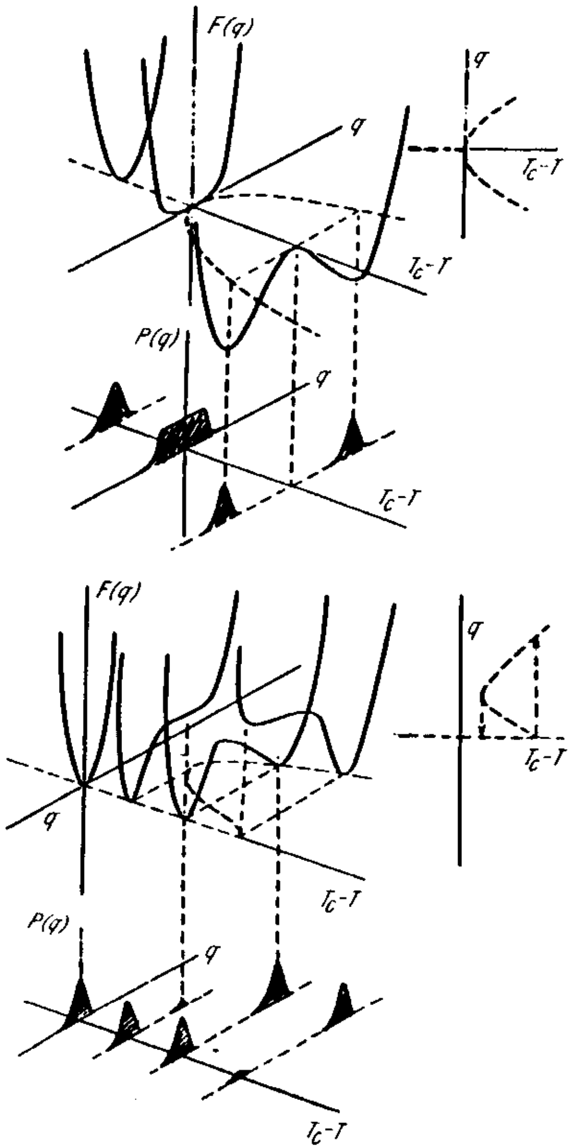

Fig. 4. Free energy and probability for 2nd and 1st order phase transition

state (population inversion). If χ is the atomic susceptibility, the constant α of Eq. (4) is

$$\alpha = \chi N - (\text{loss rate}) \tag{6}$$

and the threshold point corresponds to $\alpha = 0$.

As shown by the locus of stable points, at threshold the thermodynamic branch becomes unstable and the "coherent" branches appear. In mathematical terms, this is a bifurcation.

Still higher order bifurcations could appear, making the ordered branch unstable, and leading to new "orders".

Before discussing this multiple sequence of bifurcations it is important to decide how many degrees of freedom we have to deal with. In physics we deal in general with nonlinear equations for a field $q(x, t)$

$$\frac{\partial \vec{q}}{\partial t} = f\left(\vec{q}, \frac{\partial}{\partial \vec{x}} \vec{q}\right). \tag{7}$$

Such are the Navier-Stokes and Fourier equations for a velocity field coupled to a temperature field in a convective fluid instability. For a rectangular cell of small aspect ratio (ratio of two lateral sizes with respect to the fluid height) and for a temperature difference ΔT between lower and upper plate near the onset of the instability, Eq. (7) reduces to three coupled equations for a velocity mode and two temperature modes [4]. In suitable units, these three equations are [5]

$$\begin{aligned} \dot{x} &= -10x + 10y, \\ \dot{y} &= -y + 28x - xz, \\ \dot{z} &= (8/3)z + xy. \end{aligned} \tag{8}$$

Similarly, if we couple Maxwell equations with Schrödinger equations for N atoms confined in a cavity, and we expand the field in cavity modes, keeping only the first mode E which goes unstable, this is coupled with the collective variables P and describing the atomic polarization and population inversion as follows [2, 3]

$$\begin{aligned} \dot{E} &= -kE + gP, \\ \dot{P} &= -\gamma_\perp P + gE\Delta, \\ \dot{\Delta} &= -\gamma_\parallel(\Delta - \bar{\Delta}) - 2g(P^*E + PE^*), \end{aligned} \tag{9}$$

where k, $\gamma_\perp$, $\gamma_\parallel$ are the loss rates for field, polarization and population respectively, g is a coupling constant and $\bar{\Delta}$ the population inversion which would be established by the pump mechanism in the atomic medium, in the absence of coupling. While the first of Eqs. (9) comes from Maxwell equations, the two others imply the reduction of each atom to the levels which are resonantly coupled with the field, that is, a description of each atom in an isospin space of spin $\frac{1}{2}$. The last two equations are Bloch equations which describe the spin precession. Therefore, Eqs. (9) are called Maxwell-Bloch equations.

2. Dissipative Systems–Strange Attractors–Description of Chaos

Equations (8) and (9) are phenomenological. The presence of loss rates means that three relevant degrees of freedom are in contact with a "sea" of other degrees of freedom. In principle, they could be deduced from microscopic equations by suitable statistical reduction techniques. The fluctuation-dissipation theorem would impose the addition of stochastic forces.

However, we show that for $N \geqslant 3$ degrees of freedom, deterministic chaos may be reached in nonlinear equations as (8) or (9) without consideration of stochastic forces. These latter ones would modify some details of the phenomena, without relevant changes in the qualitative picture.

In a dissipative system there is a contraction of the phase space volume. If at time $t = 0$ the ensemble of initial conditions is confined in a hypersphere of radius E, at time t the volume will be (referring to the principal axis)

$$V(t) = \epsilon^N \exp\left(\sum_1^N \lambda_i t\right) \tag{10}$$

where the growth rates λ_i are the Lyapunov exponents. The contraction requirement means

$$\sum_1^N \lambda_i < 0. \tag{11}$$

Now, if we start from a single point at $t = 0$ (well determined initial condition) a single trajectory emerges, and on it we have obviously $\lambda = 0$.

For $N = 1$, Eq. (11) imposes $\lambda_1 < 0$, hence there is no trajectory. Indeed, the asymptotic volume can only be 0-dimensional, that is, a single point, hence we have only a stationary solution.

For $N = 2$, if $\lambda_1 < 0$, it may be $\lambda_2 < 0$ (no trajectory) but also $\lambda_2 = 0$, that is, the final volume is 1-dimensional (limit cycle) and we have a periodic oscillation.

For $N = 3$, besides points (λ_1, λ_2, λ_3 all negative) and limit cycles (λ_1, λ_2 negative, $\lambda_3 = 0$) we may have $\lambda_1 < 0$, $\lambda_2 = 0$, $\lambda_3 > 0$, with $\lambda_3 > |\lambda_1|$ to satisfy Eq. (11). This means that in direction 3 we have a stretching from ϵ to $\epsilon \exp(\lambda_3 t)$. Even if two initial conditions are very near the representative points after a long time will be largely distant. This sensitive dependence on the initial conditions (asymptotic instability) was already pointed out by Poincaré in 1890 [6] in his investigations on the gravitational 3-body problem and it is a limit to the long term stability of satellite trajectories.

The asymptotic phase space locus (after a long transient) for Lorenz equations (8) is well known. That locus attracts all neighboring initial conditions because of the compression of the phase volume peculiar of dissipative systems. It is then an *attractor*, as the fixed point for $N = 1$ or the limit cycle for $N = 2$. But nearby points at a given time must diverge after a long interval, because of $\lambda_3 > 0$. Hence the attractor will never close on itself and it is called *strange*.

The unpredictable behavior of paths started from initial conditions specified with an arbitrary (but finite) precision is a fundamental obstacle to long-term nonprobabilistic forecasting. E. Lorenz called this the "butterfly effect": if the atmosphere is described by a dynamic system with a strange attractor, even a tiny change (as that produced by the motion of butterfly wings) has catastrophic consequences for long-term weather forecasting.

This is why computers can produce only a sufficiently short realization of the path of a dynamic system with one (or more) $\lambda > 0$ (of course, the machine may go on computing, but, for large t, the path is no longer related to the initial segment).

As for the physical realizability of strange attractors, or deterministic chaos, Eqs. (9) indicate that lasers are candidated for large varieties of situations. As one changes the atomic species ($g, \gamma_\perp, \gamma_\parallel$) the pump rate ($\bar{\Delta}$) or the losses of the e.m. cavity (k). On the other hand it is well known that commercial laser sources are good examples of stable dynamical systems. The main reason is that of time scales. As shown by the coefficients of Eqs. (8), a strange attractor is obtained when the damping rates of x, y, z are comparable.

On the contrary for noble gas lasers (Ne, A) the atomic damping rates are much faster ($\gamma_\perp \sim \gamma_\parallel \sim 10^8 \div 10^9\, s^{-1}$) than the field loss rates ($k \sim 10^6 \div 10^7\, s^{-1}$). Hence the second and third of Eqs. (9) can be solved at equilibrium ($\dot{P} = \dot{\Delta} = 0$) with respect to the rather slow variations of E and substitution into the first yields a single nonlinear dissipative equation $\dot{E} = f(E)$ which allows only for a fixed point. The procedure is called adiabatic elimination [2] of the fast variables, which are slaved by the slow variable. This latter one can be considered as the only relevant dynamical variable (order parameter), as it was implicit in the heuristic considerations of Fig. 3.

As we scan most atomic or molecular species radiating in the visible or in the infrared, it is practically impossible to locate one whose rates satisfy Lorenz conditions.

We used a different approach. First we chose a molecular transition ($\lambda = 10\, \mu m$, CO_2) where relaxation of the excited state is very long ($\gamma_\parallel \sim 10^3\, s^{-1}$) so that we can adiabatically eliminate only P and we have to keep two equations. Further we add an external driving force, by periodically modulating the losses

$$k(t) = k_0(1 + m \cos \Omega t). \qquad (12)$$

If we solve the linear stability problem for the two remaining equations for E and Δ, we do not have limit cycle but a point attractor, since the associated frequencies are damped.

Applying a small perturbation, the response goes as $e^{\eta t}$ with (for $\bar{\Delta}$ twice the threshold value)

$$\eta = \eta_R + i\eta_I = -\gamma_\parallel \pm i\sqrt{k\gamma_\parallel}. \qquad (13)$$

We now fix Ω of Eq. (12) around $\sqrt{k\gamma_\parallel}$. This way, we excite a nonlinear resonance of the dynamical system and obtain a chaotic behavior. Details are given in Sect. 3.

If $f(t)$ is the physical realization of a deterministic system we try to fit the experimental points $(f_i(t_i))$ with the theoretical model. If $f(t)$ is a stochastic process the information is contained in the joint probability density $W_n(f_1(t_1), \ldots, f_n(t_n))$ of finding the values f_1 at t_1, etc. or in the correlation functions $\langle f_1(t_1), f_2(t_2), \ldots, f_n(t_n)\rangle$ (brackets are ensemble averages) [8, 9]. In both cases there are well established experimental techniques and algorithms for extracting useful information, but they are both limit cases.

It appears nowadays that the overwhelming majority of relevant situations in many-body physics (from plasmas and fluid dynamics to lasers, biology and meteorology) corresponds to deterministic chaos.

Being a rather new area of investigations, the first approaches are qualitative: either geometry of the dynamic flows in phase space, or Poincaré sections of the flow. These are particularly relevant since for a suitable choice of the hyperplane which cuts the flow with a specific constraint, the Poincaré section is particularly simple for deterministic flows and a complexity in it is an indicator of a strange attractor.

A more quantitative way of appreciating the passage from deterministic to chaotic behavior is the observation of power spectra. For deterministic systems, they are made of discrete lines, implying a finite recurrence time. Appearance of chaos is marked by the onset of a continuous spectral component. This however is a necessary, but not sufficient condition for chaos, since it is common also to purely random systems. Indeed the spectrum is the Fourier transform of the two-point correlation function (or first cumulant) which is a sufficient characterization only for Gaussian processes. Since we are away from thermal equilibrium, we expect in general strong deviations from Gaussianity with relevant contributions in higher cumulants.

A more quantitative approach will be discussed later below.

3. Some Experimental Cases: Coexistence of Many Attractors and Low Frequency Spectra

Here I discuss four experiments on the onset of chaos performed by my group. The first refers to an electronic nonlinearity, the others to CO_2 laser systems.

Besides showing the application of the above-mentioned experimental techniques, we give evidence of the simultaneous coexistence of many attractors for the same values of the external (or control) parameters. This phenomenon was called "generalized multistability" because it is a generalization of the coexistence of more than one fixed point for the same input.

a) Electronic Nonlinearity

Let us consider a dynamic system, ruled by the equation

$$\dot{\vec{x}} = \vec{F}(\vec{x}; \vec{\mu}) \tag{14}$$

where $\vec{x}$ is an n-dimensional vector, $\vec{F}$ a nonlinear function and $\vec{\mu}$ an m-dimensional control parameter.

We study the equilibrium solutions

$$\vec{F}(\vec{x}; \vec{\mu}) = 0 \tag{15}$$

for different $\vec{\mu}$. For some critical $\vec{\mu}$, some stationary solutions may switch from stable to unstable (bifurcations). An example is the laser threshold.

We are not interested in the general treatment of bifurcations, but just in how they may lead in some systems to turbulence, or chaos. One of the indicators of turbulence is the appearance of a continuous power spectrum.

Before 1963, the Landau-Hopf model [10], based on mode-mode coupling in a fluid due to the nonlinear hydrodynamic equations, hypothesized the generation of a large amount of uncommensurate frequencies, which eventually accumulated into a continuum.

In 1963 Lorenz [5] showed that three coupled nonlinear equations were enough to reach chaos. The three ordinary equations were truncated versions of field equations with drastic cut-offs due to the boundary conditions, as said above.

Equivalent to three coupled equations is a system of two first order equations (or second order equations) plus an external modulation. An example is the driven Duffing oscillator

$$\ddot{x} + \gamma\dot{x} - \omega_0^2 x + \beta x^3 = A \cos \omega t \tag{16}$$

which can be experimentally realized with an electronic oscillator [11].

Eq. (16) is equivalent to 3 coupled equations

$$\begin{aligned} \dot{x} &= y, \\ \dot{y} &= -\gamma y + \omega_0^2 x - \beta x^3 + A \cos z, \\ \dot{z} &= \omega. \end{aligned} \tag{17}$$

For a suitable sequence of parameters $\vec{\mu}$ (either modulation amplitude A or frequency ω) it gives a sequence of subharmonic bifurcations leading eventually to chaos as shown in Fig. 5.

The sequence of subharmonic bifurcations corresponds to the successive appearance of periods $T = 2\pi/\omega$, $2T$, $4T, \ldots, 2^n T$ in the output.

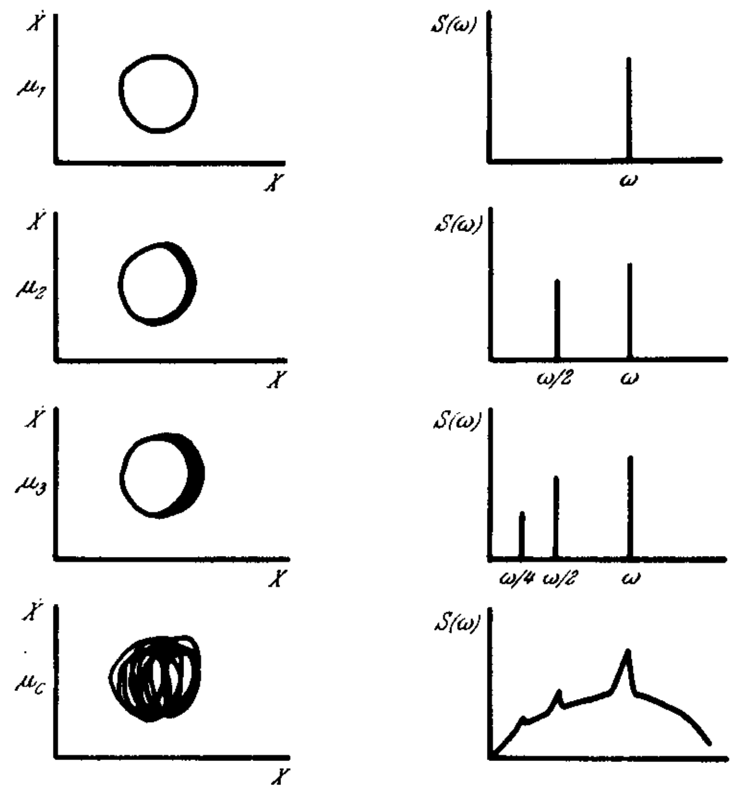

Fig. 5. Phase space plots $(\dot{x}, x)$ and power spectra $S(\omega)$ for different control parameters

If we call μ_n the value of the parameter at which the period $2^n T$ appears, then the following relation is verified

$$\delta \equiv \frac{\mu_{n+1} - \mu_n}{\mu_{n+2} - \mu_{n+1}} \underset{n \gg 1}{\rightarrow} 4.669\ldots \quad (18)$$

This number has been shown by Feigenbaum [12] to be universal.

If, in the space $(\dot{x}, x, t)$ one considers the discrete transformation from the point $(\dot{x}, x)$ at time t to the point $(\dot{x}, x)$ at time $t + T$ after integration of Eq. (17) over that interval, one has the discrete mapping

$$\vec{x}_{t+T} = \vec{f}(\vec{x}_t). \quad (19)$$

Such a correspondence is illustrated in Fig. 6. Plotting all crossing points with the constant-phase planes on a single plane, we have a stroboscopic,

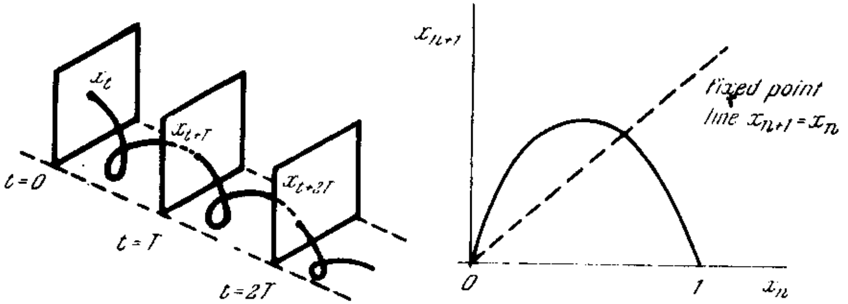

Fig. 6. Trajectory in 3-*D* phase space (solid line) and direct mapping $x_t \rightarrow x_{t+T}$. Example of quadratic map

or Poincaré, map. Of course, having performed a time integral, one has reduced the three-dimensional differential problem (17) to a two-dimensional recurrence (19). In many relevant cases the points of the Poincaré map accumulate over an almost one-dimensional manifold. Since the interesting bifurcations are associated with a change of slope, the 1-*D* map can be studied around a maximum. Thus, one-dimensional quadratic maps as

$$x_{n+1} = \mu x_n (1 - x_n) \quad (20)$$

display many features of Eq. (15).

One can develop a straightforward set of transformations using discrete maps [13, 14]. For instance, the second iterate is

$$x_{t+2T} = f(x_{t+T}) = f(f(x_t)) = f^{(2)}(x_t)$$

and a fixed point is ruled by the equation

$$x_{t+T} = x_t = f(x_t).$$

Of course, a fixed point in the map does not mean a single equilibrium point like for the differential equation, but a limit cycle of period T, whereby the position in phase space goes onto itself at each T. A period $2T$ would appear as a solution of the equation

$$x_{t+2T} = x_t = f^{(2)}(x_t)$$

and so on. Feigenbaum [12] has evaluated his δ value by showing that, in such cascades of period doublings, the local structure of the attractor is reproduced at a rescaled size in successive bifurcations, with the rescaling parameter being a universal constant.

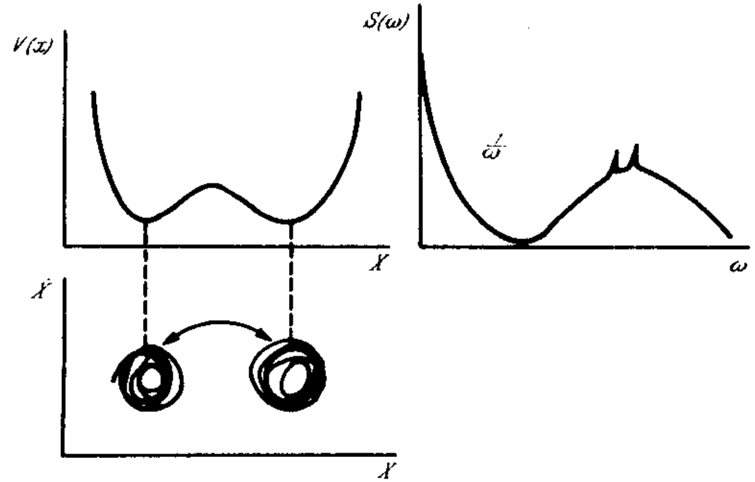

Fig. 7. *a* Bistable potential $V(x)$. Coexistence of two strange attractors in $(\dot{x}, x)$ with possible mutual jumps induced by external noise (line with arrows). *b* Birth of $1/\omega$ branch in power spectrum associated with the above jumps

Noise is not essential (deterministic chaos), but if we add it, the number of subharmonic bifurcations before chaos becomes smaller and smaller. This can be put in terms of a scaling law where the variance of the external noise appears somewhat as a modification of the control parameter [15, 16]. For low excitation values μ, depending on the initial conditions, we have two independent attractors, confined in the two valleys of the Duffing potential as shown in Fig. 7. Increase μ until they both get strange. Now, addition of a small random noise may trigger jumps from one to the other. These jumps give a low frequency divergence in the power spectrum [11]. They couple two strange attractors, otherwise independent.

b) Chaos in Quantum Optics–I. Case

After the first evidence of the jumping phenomenon, a similar effect was observed in a modulated CO_2 laser [7]. It corresponds to a set of 3 coupled rate equations, with time dependent cavity losses $k(t)$, that is, calling Δ the populations inversion and n the photon number, to

$$\dot{\Delta} = R - 2Gn\Delta - \gamma_{\parallel}\Delta,$$
$$\dot{n} = Gn\Delta - k(t)n, \qquad (21)$$

where $k(t)$ is given by Eq. (12).

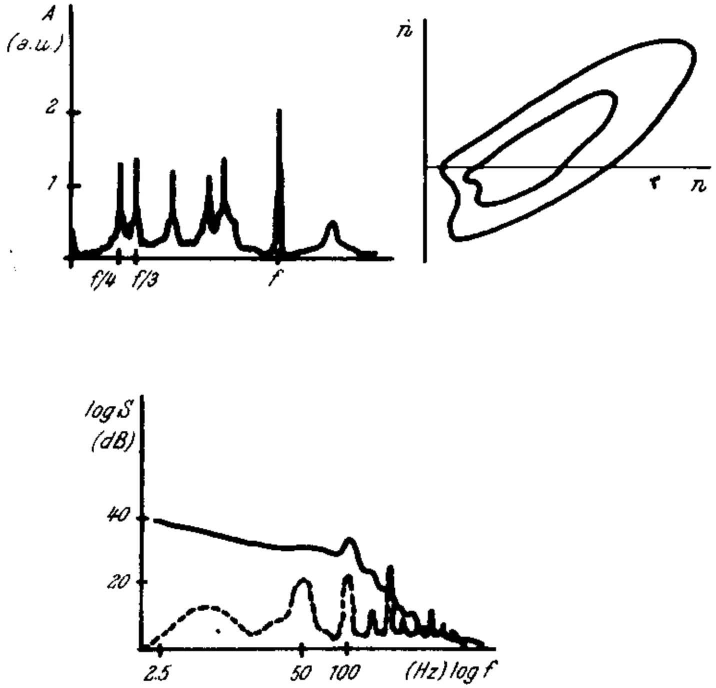

Fig. 8. Bistability in a CO_2 laser with loss modulation with coexistence of two attractors (period 3 and 4, respectively), *a* spectra of stable attractors, *b* phase space plots, *c* comparison between the low frequency cut-off, when the two attractors are stable, and the low frequency divergence, when the two attractors are strange

Fig. 8 shows bistability, that is, simultaneous coexistence of two attractors corresponding respectively to $f/4$ and $f/3$ subharmonic. Increasing the modulation depth m, the attractors become strange and the spectrum shows a low frequency spectral divergence (Fig. 8c) so that the

extension of turbulence considerations to more than one attractor (multistable situations) seems a successful conjecture.

These jump spectra have been analyzed for a suitable map allowing for two independent attractors [17]. On the other hand, low frequency spectra are sometimes observed for a single attractor, when it is made of two sub-regions weakly coupled (deterministic diffusion) [18]. In both cases these frequencies have a power law behavior $f^{-\alpha}$ over a broad frequency range, with α around 1. This resembles the so-called $1/f$ noise, encountered in many physical circumstances.

With reference to a region of the parameter space of the Duffing equation where many (i.e. 5) attractors coexist, we measure the mean escape time T from one attractor, versus the amplitude σ of an applied noise.

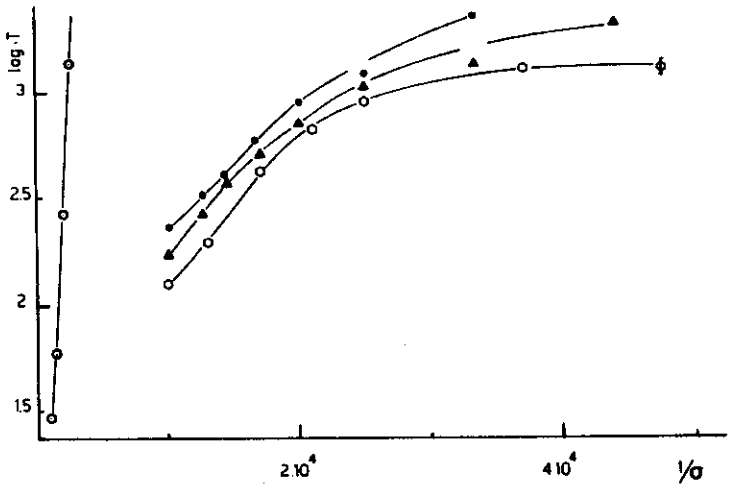

Fig. 9. Mean escape time T from an attractor versus the inverse amplitude $1/\sigma$ of the applied noise for different control parameters below and above the crisis value A_c

Fig. 9 shows $\log T$ versus $1/\sigma$ for different values ($A_1 < A_2 < A_3 < A_4$) of the driving amplitude A at fixed frequency [19]. $A_3 = A_c$ is the parameter at which the period 7 undergoes crisis [20], that is, the representative point escapes from the attractor after an infinite time, in the absence of noise.

For $A_4 > A_c$ even a zero noise ($1/\sigma \to \infty$) yields a finite escape time as it is evident from the corresponding saturated plot. For $A < A_c$, $T \to \infty$ as $\sigma \to 0$, the more the smaller is A, as shown by comparison between A_1 and A_2. The finite escape time across a bounded region for $A > A_c$ corresponds to the deterministic (noise-free) diffusion discussed elsewhere. On the contrary, for $A < A_c$, where the attractor is structurally stable, the uniqueness theorem for solutions of a differential system forbids the phase point from leaving the attractor, unless we apply external noise. This is the phenomenon of noise induced jumps already reported experimentally [11, 7] and simulated with a one-dimensional map [17]. Notice that both for $A > A_c$ and $A < A_c$ around the crisis region the large escape times give low frequency power spectra which are qualitatively similar. The essential difference is that for $A < A_c$ no jumps occur in the absence of noise.

It is apparent from Fig. 9 that one can have the same T for different A's, adjusting the noise amplitude. This may be expressed in terms of a scaling relation [19] as given for other chaotic scenarios [15, 16].

c) Chaos in Quantum Optics–II. Case

Rather than acting upon a CO_2 laser with an external modulation, we can inject a field from another laser. If the injecting frequency is away by $\Delta\omega$ from the "natural" frequency of the main laser, we must account for Re $E \equiv X$ and Im $E \equiv y$ as two independent dynamical variables which, coupled with the population, give $N = 3$. Furthermore, if $\Delta\omega$ is around the eigenvalues the nonlinear resonance will give rise to chaos, as discussed in ref. [21].

d) Chaos in Quantum Optics–III. Case

In order to decouple the injecting from the main laser, we have realized a ring configuration (Fig. 10) where forward and backward waves

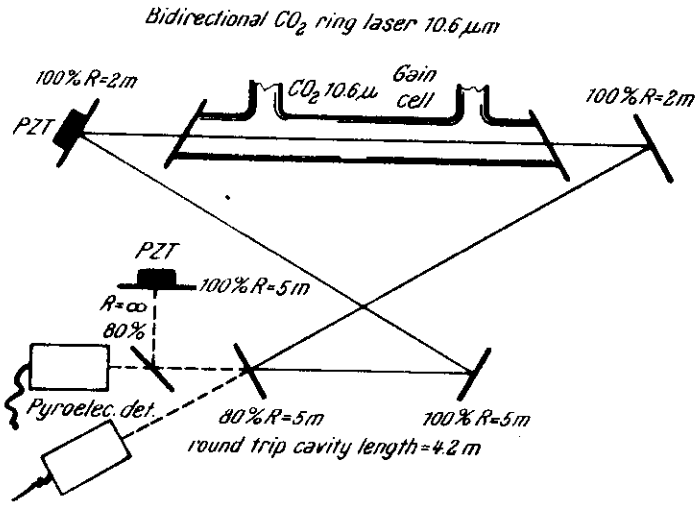

Fig. 10. Bidirectional CO_2 ring laser

have different propagation outside the cavity. As we modify the laser parameter we observe bistability (either mode quenching the other), periodic pulsations and eventually chaos. At variance with a dye ring laser [23], where adiabatic elimination of atomic variables yields a dynamic system with $N = 2$ (the two countergoing field amplitudes), for the CO_2 laser we must add in a relevant way the population amplitude. In this configuration, this implies at least three more degrees of freedom, namely Δ_0 (the uniform component of inversion) and $\Delta_{\pm 2k}$ (the second harmonic population grating induced by saturation which couples the two countergoing fields). Hence we can have a deterministic chaos, which would be forbidden in ref. [23]. We have reached a satisfactory agreement between experiments and numerical solutions of the equations.

4. Conclusions

By a description of a few experimental cases we have shown that quantum optical devices, being made of a small, and in any case controllable, number of degrees of freedom are the best systems to test deterministic chaos, without having to recur to questionable truncation procedures as in hydrodynamics.

For brevity reasons, this presentation has limited the experimental evidence to phase space plots or to power spectra. More powerful information retrieval techniques are provided by measurement of the fractal dimensions of the chaotic attractors. This is equivalent to studying higher order correlation functions [24], hence going beyond the limited information of the power spectrum.

These techniques have been used in our experimental investigations [22] and they seem at this moment the most sensible tool for distinguishing order, deterministic chaos, and purely stochastic randomness.

References

[1] Arecchi, F. T.: Photocount Distributions and Field Statistics (Proc. E. Fermi, School 1967), in: Quantum Optics (Glauber, R. J., ed.). New York: Academic Press 1969.
[2] Haken, H.: Synergetics. Berlin-Heidelberg-New York: Springer 1977.
[3] Arecchi, F. T.: Experimental Aspects of Transition Phenomena in Quantum Optics (Proc. XVIIth International Solvay Conference on Physics, 1978), in: Order and Fluctuations in Equilibrium and Nonequilibrium Statistical Mechanics (Nicolis, G., *et al.*, eds.). New York: J. Wiley 1981.
[4] Chandrasekhar, S.: Hydrodynamics and Hydromagnetic Stability. London: Oxford University Press 1961.
[5] Lorenz, E.: J. Atmos. Sci. **20**, 130 (1963).
[6] Poincaré, H.: Traité de mécanique céleste. Dover 1957.

[7] Arecchi, F. T., Meucci, R., Puccioni, G., Tredicce, J.: Phys. Rev. Lett. 49, 1217 (1982).
[8] Shannon, C. E., Weaver, W.: The Mathematical Theory of Information. University of Illinois Press 1962.
[9] Wang, M. C., Uhlenbech, G. E.: Rev. Mod. Phys. 17, 323 (1945).
[10] Landau, L., Lifshitz, E.: Statistical Physics. Oxford: Pergamon Press 1958.
[11] Arecchi, F. T., Lisi, F.: Phys. Rev. Lett. 49, 84 (1982).
[12] Feigenbaum, M. J.: J. Stat. Phys. 19, 25 (1978); 21, 669 (1979).
[13] May, R. M.: Nature 261, 459 (1979).
[14] Collet, P., Eckmann, J. P.: Iterated Maps. Basel: Birkhäuser 1980.
[15] Crutchfield, J. P., Huberman, B. A.: Phys. Lett. 77A, 407 (1980).
[16] Shraiman, B., Wayne, K., Martin, P. C.: Phys. Rev. Lett. 46, 935 (1981).
[17] Arecchi, F. T., Badii, R., Politi, A.: Phys. Rev. A (1984).
[18] Geisel, T., Nierwetberg, J.: Phys. Rev. Lett. 48, 7 (1982); Grossman, S., Fujsaka, H.: Z. Phys. B48, 261 (1982).
[19] Arecchi, F. T., Badii, R., Politi, A.: Phys. Lett. 103A, 3 (1984).
[20] Grebogi, G., Ott, E., Yorke, Y.: Phys. Rev. Lett. 49, 1507 (1982).
[21] Arecchi, F. T., Lippi, G., Puccioni, G., Tredicce, J.: this same workshop.
[22] Arecchi, F. T., Lippi, G. L., Tredicce, J., Abraham, N. B.: Invited talk at the XIIIth Int. Conf. on Quantum Electronics, Los Angeles, Cal., June 18–21, 1984.
[23] Roy, R., Mandel, L.: Opt. Commun. 34, 133 (1980).
[24] Grassberger, P., Procaccia, I.: Physica 9D, 189 (1983).

Printed in Austria

(10)

[redacted]

FROM: F.T. ARECCHI - ORDER & CHAOS IN PHYSICS - 1984

5. *Information content in a turbulent system*

In Sec. 2 and 3 we have shown how to characterize a nonlinear dynamical system by Lyapunov exponents, phase space plots and their Poincaré sections, and power spectra. It is difficult to extract precise values of Lyapunov numbers from a set of experimental data, even in theretical models, where it requires a very large amount of computer time [23]. The geometry of phase space is only a qualitative approach. The power spectra are an incomplete description of a hierarchy of correlation functions (the two points correlation, sufficient only for Gaussian stochastic processes).

Furthermore, a low resolution picture of a strange attractor or a continuous power spectrum is unable to tell whether a given system is random (complete filling of an N-dimensional region of a N-dimensional phase space) or just complex (deterministic chaos as the accumulation point of a sequence of bifurcations, more «predictable» than pure randomness). In this second case, the strange attractor is a manifold with dimensions lower than N.

It is clear from Shannon's [8] interpretation of entropy that order is basically an information theoretic concept (unlike the superficially similar concept of symmetry which is group theoretic). Accordingly, two of the most basic properties of dissipative chaotic systems are related to information: the Kolmogorov [24] (or «metric») entropy K and the Renyi-Balatoni [25] information dimension σ.

Both are related to the information $I(\varepsilon,T)$ gained by observing a trajectory of the system with precision ε during a time T. Here, we assume that the structure of the attractor is already known, so that the observation gives new information only on the actual trajectory.

The Kolmogorov entropy is obtained by observing a very long time,

$$k = \lim_{\epsilon \to 0} \lim_{T \to \infty} \frac{I(\epsilon, T)}{T}. \qquad (22)$$

The precision ε is here the uncertainty in the measurement of any of the coordinates of the state vector $\vec{x}$. Notice that the infinite-time limit is taken first. The information for a given precision ε increases linearly in time, and the rate of increase tends towards a finite constant for infinite precision.

This should be compared to ordered deterministic motion, where

$$\lim_{T \to \infty} \frac{I(\epsilon, T)}{T} = 0 \qquad \text{(order)} \qquad (23)$$

and to systems subject to random noise where

$$\lim_{T \to \infty} \frac{I(\epsilon, T)}{T} \propto \ln \frac{1}{\epsilon} \underset{\epsilon \to 0}{\to} \infty \,. \qquad \text{(stochastic)} \qquad (24)$$

The information dimension σ is defined by the information obtained in an observation during a finite time T (consisting eventually of a single-time measurement, $T = 0$)

$$\sigma = \lim_{\epsilon \to 0} \frac{I(\epsilon, T = 0)}{\ln 1/\epsilon} \,. \qquad (25)$$

The importance of K and σ derives in particular from the fact that they are invariants. They both are related to the Lyapunov exponents λ_i ($i = 1, ...N$; N = number of directions of phase space).

One has the rigorous inequality [14]

$$K \leq \sum' \lambda_i \,, \qquad (26)$$

where the sum runs over all positive Lyapunov exponents. But it is widely accepted that this is indeed an equality for all typical attractors. In particular, there does not seem to exist any known example where eq. (26) is a strict inequality.

Eq. (26) allows very easy computation of K for models in which the equations of motion are known analytically. In experimental situations, however, neither the calculation of Lyapunov exponents nor the direct calculation of K via its definitions seems feasible.

This is different for the generalized dimensions and entropies which we shall discuss now.

The information $\bar{I}(\epsilon) = I(\varepsilon, T = 0)$ in eq. (25) is defined technically via a partitioning of the attractor into cubes of size ε. Let us call p_i the probability for an arbitrary point on the attractor to fall into cell i.

Then, $\bar{I}(\varepsilon)$ is defined as

$$\bar{I}(\varepsilon) = -\sum_i p_i \ln p_i \,. \qquad (27)$$

The order-q Renyi informations are now defined as [26]

$$\bar{I}_q(\epsilon) = \frac{1}{1-q} \ln \sum_i p_i^q \qquad (28)$$

and related order-q dimensions of the attractor can be defined as [28]

$$D_q = \lim_{\epsilon \to 0} \frac{\bar{I}_q(\epsilon)}{\ln 1/\epsilon} \,. \qquad (29)$$

Obviously, $\sigma = \lim_{q \to 1} D_q$ while $\lim_{q \to 0} D_q$ is just the Hausdorff dimension or capacity (see Appendix).

Consider $q = 2$. The sum $\sum p_i^2$ is just the probability that a pair of random points on the attractor fall into the same cube of the partitioning. Up to an ε-independent factor, this is also the chance that two arbitrary points will have a distance $\lesssim \varepsilon$. Calling this probability $C(\varepsilon)$, we expect thus

$$C(\varepsilon) \underset{\epsilon \to 0}{\sim} \varepsilon^{D_2}. \qquad (30)$$

For the practical calculation of $C(\varepsilon)$ and D_2, consider a time series $\{\vec{x}_n = \vec{x}(t + n\tau);\ \tau \text{ fixed},\ n = 1, ... M\}$. Due to the exponential divergence of near-by trajectories, some points will be essentially uncorrelated, leading to

$$C(\varepsilon) = \lim_{M \to \infty} \frac{1}{M^2} \times \left[\text{number of pairs such that}_{|\vec{x}_n - \vec{x}_m| \leq \varepsilon} \right] \qquad (31)$$

In a similar way D_q ($q \geq 3$) can be obtained from the correlations between q-tuples of points.

From the definitions it follows that

$$D_0 \geq D_1 \geq D_2 \,. \qquad (32)$$

The physical meaning can be summarized as follows (see also the Appendix).

D_0 is the Hausdorff dimension of the strange attractor. It is smaller than the dimensonality N of the phase space ($D_0 = N$ means that we are filling the phase space, that is, we have a random system). D_1 (information dimension) and D_2 (correlation dimension) depend on the density of points in different subregions of the attractor, that is, on the frequency of visitation of different regions of phase space.

For a rather precise determination of D_2 following Def. (32) we need a few thousand points. This should be compared with the 10^6 points needed to obtain convergence of the box counting algorithm used to compute D_0 along the definition (A.1).

In experiments, one has the output from a given detector, which picks one of the N components of the phase space point $\bar{X} \equiv (x_1, x_2, ... x_N)$. For sufficiently long time differences θ (embedding theorem) [29] the sequence

$$x_1(t),\ x_1(t+\theta),\ x_1(t+2\theta), ... x_1(t+m\theta)$$

has the same amount of information as the phase point provided $m \geq 2N+1$. This way, as t goes on, we can build from experimental data a 1-dimensional subspace $X_1(t)$, a 2-dimensional subspace $X_1(t), X_1(t+\theta)$ and so on. Measuring for each realization the corresponding exponents D_2 we reach a saturation. That means that we have already reached the dimensionality of the attractor and there is no reason to go further. This is illustrated in fig. 15 for the strange attractor of our Marangoni instability. It is worthwhile to notice that, just near the onset of chaos the dimensional D_2 is around 2.3, hence the topological dimension D_0 of the attractor is as D_2 or slightly larger against a total number of degrees of freedom (for a cubic centimenter of fluid) $N \sim 10^{23}$! Such low dimensional varieties show some universal character which means that once a cooperative behavior has been established, even if the system is not absolutely ordered ($D_0 = 0$ or 1) still there is a comfortable degree of predicability with respect to absolute randomness (where $D_0 = N = 10^{23}$ for our fluid!).

6. *Epistemological implications*

It is amusing that physical curricula are based on cases where $K = 0$ (as classical mechanics) or $K = \infty$ (as equilibrium thermodynamics) while almost all practical situations correspond to a finite metric entropy $0 < K < \infty$.

The recent rapid growth of the physics of order from chaos and the onset of deterministic chaos (complex trajectories extremely sensitive to initial conditions, because of asymptotic instabilities) has established a kind of interdisciplinary language based on system dynamics and independent of physical details called «synergetics» [2] or «self-organization» [31]. Indeed once a drastic decimation from 10^{23} to less than 10 in the number of relevant degrees of freedom has occurred, many microscopic details lose their relevance

It is worth to reconsider the general attitude of physicists with respect to nature.

Physics is mathematized in terms of a time evolution operator U which, acting on a set of initial data φ, transforms then into a set f at a later time, that is,

$$U\varphi = f. \tag{33}$$

Eq. (33) is used in many ways. First, if U is known from theory and φ is assigned by a suitable method, then predictions on f can be made (direct problem). This would generally be considered an easy task for a physicist, because it is an application within the realm of an established theory: like doing E.M. propagation with given boundary conditions after all the work from Maxwell to the World War II Radar investigations. Second, one can measure φ and then f at a later time, in order to establish the structure of U. This is the logical process of building a theory. The establishment of Kepler's laws was done this way, by comparing astronomical data at different times. This is the way Maxwell equations, Weinberg-Salam electroweak theory and nowadays the ambitious Grand Unification Theories have been built. It is considered the central task of a physicist. It may eventually arrive to an end when fundamental interactions have been understood [32].

This however will not signal the end of physics. Going back to the direct problem, we have seen how the mathematics of non-linearities, started by Poincaré and then overlooked for 70 years because of the excitement of microphysics (from radio-activity in the 1890's to quarks in the 1960's) has provided new vistas, including universal behaviors brought up by the global topology of phase space and not by detailed microscopic interactions.

There are still other ways of reading eq. (33). If f is measured and U is assigned from a theory, the aim is the reconstruction of the initial state φ

(third way). This is the goal of all evolutionary theories (as cosmogony). This inverse problem is affected by intrinsic instabilities [33]. They can be appreciated already in an elementary case. If U is a linear convolution, then (33) can be Fourier transformed and the inverse problem has the solution

$$\varphi(\omega) = \frac{f(\omega)}{U(\omega)} . \tag{34}$$

Now the measurement of f is performed with a finite precison and this implies errors, which are usually broad-band

$$f(\omega) = \bar{f}(\omega) + \varepsilon ,$$

where $\bar{f}(\omega)$ is bandlimited, while ε has a white spectrum (that is, it is finite as $\omega \to \infty$). As for $U(\omega)$, since it comes from a «reasonable» theory, it is in general well behaved, that is,

$$U(\omega) \underset{\omega \to \infty}{\longrightarrow} 0 .$$

Hence the reconstruction yields unphysical divergences, since

$$\varphi(\omega) \underset{\omega \to \infty}{\longrightarrow} \infty .$$

There is eventually a fourth way of doing physics, which was the dream of empiricists, that is, to trace a large set of data φ over a long time, in order to be able to make predictions on f over a reasonably long future, without having to recur to a «theory» U.

Information theory applied to physics as discussed in the previous Section seems to provide the necessary tools for this task. It is however my opinion that this latter attitude is an «asymptotic», one, which may be taken for the sake of discussion, but without a serious purpose. The physicists will continue to formulate models, as it has always been since Galileo, whatever will be the sophistication of the retrieval techniques, because his goal is not simply to provide sensible forecasts, but to understand Nature.

(13)

APPENDIX

On fractal dimensions

For a dynamics system with an N-dimensional phase space, let $n(\epsilon)$ be the number of N-dimensional balls of radius ϵ required to cover an attractor. The capacity, or fractal dimension [34] is

$$D_0 = \lim_{\epsilon \to 0} \frac{\log n(\epsilon)}{\log 1/\epsilon} \tag{A.1}$$

When a set is «simple», for example, a limit cycle or a torus, the fractal dimension is an integer equal to the topological dimension.

To understand the meaning of the fractal dimension, suppose that the N coordinates of a dynamical system are measured by an instrument incapable of resolving values separated from each other by less than ϵ. The instrument thus induces a partition that divides the phase space into elements of equal volume. To an observer whose only a priori knowledge is a list of the $n(\epsilon)$ partition elements that cover the attractor, the amount of new information gained upon learning that the phase point describing the state of the system is in a given partition element is $\log n(\epsilon)$. If the resolution of the measuring instrument is increased, the number of partition elements needed to cover the attractor goes up roughly as ϵ^{-D_0}. Thus, assuming that all partition elements are equally likely, for small ϵ the amount of new information obtained in a measurement is roughly

$$I = \log n(\epsilon) \approx D_0 \log 1/\epsilon . \tag{A.2}$$

For most chaotic attractors, however, the elements of a partition do not have equal probability. Assume that each element of a partition has probability P_i. On the average, the amount of information gained in a measurement by an observer whose only a priori knowledge is the distribution of probabilities $\{P_i\}$ is

$$I(\epsilon) = -\sum_{i=0}^{n(\epsilon)} p_i \log p_i \tag{A.3}$$

(44)

This leads to a generalization of the fractal dimension:

$$\sigma \equiv D_1 = \lim_{\epsilon \to 0} \frac{I(\epsilon)}{\log 1/\epsilon} \qquad (A.4)$$

This dimension was originally defined by Balatoni and Renyi[26] in 1956. They refer to it simply as the «dimension of a probability distribution». In order to avoid confusion with other dimensions, however, we will refer to this as the information dimension. Since $\log n(\epsilon) \geq I(\epsilon)$, the fractal dimension D_0 is an upper bound for the information dimension D_1.

REFERENCES

1. F.T. ARECCHI, «Photocount distribution and field statistics» (Proc. E. Fermi, School 1967) in *Quantum Optics* ed. by R.J. Glauber, Academic Press, 1969.
2. H. HAKEN, *Synergetics*, Springer Verlag 1977.
3. F.T. ARECCHI, «Experimental Aspects of Transition Phenomena in Quantum Optics» (Proc. XVIIth International Solvay Conference on Physics, 1978) in a *Order and Fluctuations in Equilibrium and Nonequilibrium Statistical Mechanics* ed. by G. Nicolis et all., J. Wiley, 1981.
4. S. CHANDRASEKHAR, *Hydrodynamics and Hydromagnetic Stability*, Oxford U. London 1961.
5. E. LORENZ, J. Atmos. Scie. *20*, 130 (1963).
6. H. POINCARÉ, Traité de mecanique celeste, Dover 1957.
7. F.T. ARECCHI, R. MEUCCI, G. PUCCIONI, J. TREDICCE, Phys. Rev. Lett. *49*, 1217 (1982).
8. C.E. SHANNON and W. WEAVER, *The Mathematical Theory of Information* (Univ. of Illinois press, 1962).
9. M.C. WANG and G.E. UHLENBECH, Rev. Mod. Phys. *17*, 323 (1945).
10. L. LANDAU and E. LIFSHITZ, Statistical Physics, Pergamon Press, 1958.
11. F.T. ARECCHI and F. LISI, Rev. Lett. *49*, 94 (1982).
12. M.J. FEIGENBAUM, J. Stat. Phys: *19*, 25 (1978); *21*, 669 (1979).
13. R.M. MAY, Nature, 261, 459 (1979).
14. P. COLLET and J.P. ECKMANN, Iterated Maps, Birkhauser (1980).
15. J.P. CRUTCHFIELD and B.A. HUBERMAN, Phys. Lett. *77A*, 407, (1980).
16. B. SHRAIMAN, K. WAYNE and P.C. MARTIN, Phys. Rev. Lett. *46*, 935 (1981).
17. F.T. ARECCHI, R. BADII, A. POLITI, Phys. Rev. *A* (Rap. Comm.) (Feb. 1984).
18. T. GEISEL and J. NIERWETBERG, Phys. Rev. Lett. *48*, 7 (1982); S. GROSSMAN and H. FUJSAKA, Z. Phys. *B48*, 261 (1982).
19. E.W. MONTROLL and M.F. SCHESINGER, Proc. Nat. Acad. Sci. (USA) *79*, 3380 (1982).